Computers and Concrete, Vol. 8, No. 1 (2011) 43-57
DOI: http://dx.doi.org/10.12989/cac.2011.8.1.043

Force-deformation behaviour modelling of cracked reinforced concrete by EXCEL spreadsheets

Nelson Lam*[1], John Wilson[2] and Elisa Lumantarna[1]

[1]*Department of Civil & Environmental Engineering, c/o School of Engineering, University of Melbourne, Parkville, 3010, Australia*
[2]*Swinburne University of Technology, Hawthorne, Victoria, Australia*

(Received July 27, 2009, Accepted November 11, 2009)

Abstract. Force-deformation modelling of cracked reinforced concrete is essential for a displacement-based seismic assessment of structures and can be achieved by fibre-element analysis of the cross-section of the major lateral resisting elements. The non-linear moment curvature relationship obtained from fibre-element analysis takes into account the significant effects of axial pre-compression and contributions by the longitudinal reinforcement. Whilst some specialised analysis packages possess the capability of incorporating *fibre-elements* into the modelling (e.g., RESPONSE 2000), implementation of the analysis on EXCEL is illustrated in this paper. The outcome of the analysis is the moment-curvature relationship of the wall cross-section, curvature at yield and at damage control limit states specified by the user. Few software platforms can compete with EXCEL in terms of its transparencies, versatility and familiarity to the computer users. The program has the capability of handling arbitrary cross-sections that are without an axis of symmetry. Application of the program is illustrated with examples of typical cross-sections of structural walls. The calculated limiting curvature for the considered cross-sections were used to construct displacement profiles up the height of the wall for comparison with the seismically induced displacement demand.

Keywords: deformation modelling; cracked reinforced concrete; deflection; EXCEL; spreadsheets; fibre element analysis; RESPONSE 2000.

1. Introduction

Fibre-elements have been developed as a technique for modelling the non-linear post-yield response behaviour of composite structures such as reinforced concrete in the cracked state to extreme loading (Spacone *et al.* 1996a and 1996b, Monti *et al.* 2000). This modelling approach is generally not used in day-to-day engineering practices although it is featured in some finite element software (e.g., FEAP 1998) and a few special purpose computer programs developed in the course of a research project (e.g., RESPONSE 2000). A more "user-friendly" program has been developed recently for modelling the sectional properties of reinforced concrete columns with circular and square cross-sections (CUMBIA 2007).

The purpose of this paper is to introduce a program written on spreadsheets for undertaking similar analyses on reinforced concrete sections of arbitrary geometry including those found in reinforced concrete structural walls (Figs. 1(a)-1(f)). All sides of the cross-section must be parallel

* Corresponding author, Ph.D., E-mail: ntkl@unimelb.edu.au

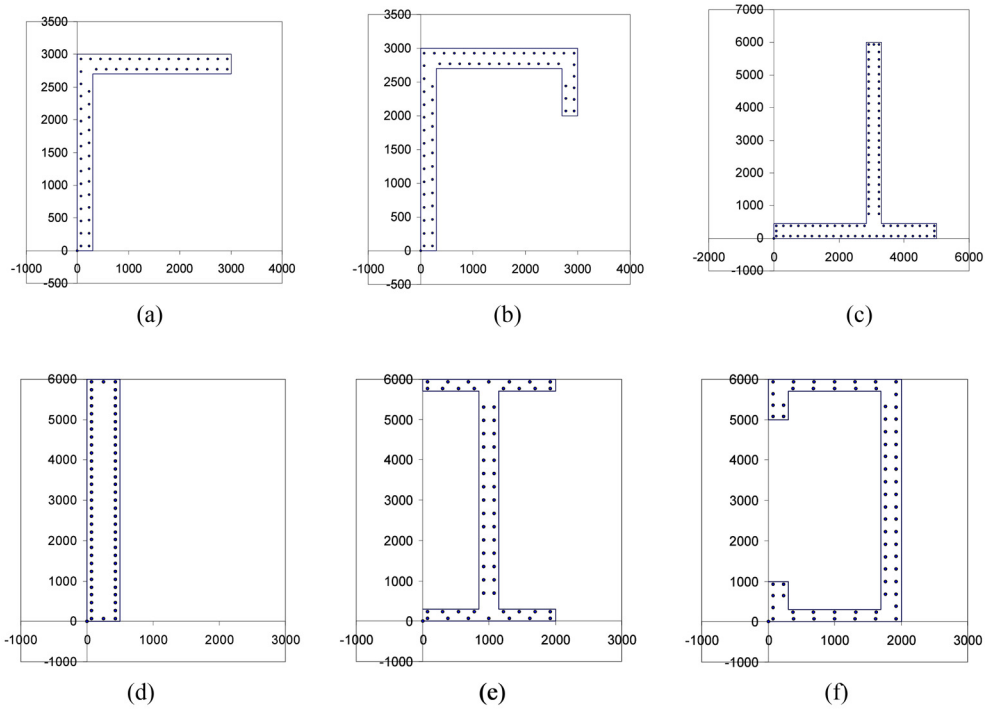

Fig. 1 (a)-(f) Spreadsheet images of wall cross-sections

to either the *X* or *Y* axis. It is noted that the analysis is based on uni-axial bending about the *X* axis. Asymmetrical bending and torsional actions on the wall resulted from asymmetry about both axes are assumed to be fully constrained by other lateral resisting elements in the building and hence their effects are not taken into account by the analysis. For the convenience of the users, all Input/ Output to the program are done on the *User Interface* spreadsheet placed at the beginning of the file (Section 2). The computations are conducted on the other eleven spreadsheets. Key features with programming for the computations will also be described to facilitate readers developing their own program customizing specific needs (Section 3). Example moment-curvature relationships generated by the program will be presented for comparison with simulations obtained from the well known program RESPONSE 2000 (Section 4). Applications of the program in assessing the potential strength-displacement capacity of reinforced concrete (RC) walls in countering seismic excitations and other forms of extreme loading will also be illustrated (Section 5).

2. User interface of program

The *USER INTERFACE* spreadsheet as shown in Fig. 2 is divided into the following zones : (i) Input of the concrete cross-section (ii) Input of the reinforcement details and (iii) Output summary which includes reporting of the moment-curvature relationship. A moment-curvature diagram is placed below the summary table (and is shown in Fig. 5). Fields for input by the user are identified by yellow patches on the "user-interface" worksheet (Fig. 2).

2.1 Input of geometry of wall cross-section and concrete properties

The geometry of the wall cross-section is input by the user specifying the *Cartesian* co-ordinates for each of the corners of the section beginning with the bottom left-hand corner which is by default node no. "1". The numbering of the other nodes is then assigned by following the perimeter of the cross-section in anti-clockwise sense as shown in Fig. 3. The gross cross-sectional area of the wall is automatically calculated and shown below the table of nodal co-ordinates. Other input parameters to be keyed in are the characteristic strength of the concrete (f_c') and the applied axial force (N).

The directivity of each side of the cross-section is automatically identified by the program (Fig. 3). For example, the directivity of the side of the cross-section in between node "1" and "2" is defined as positive (as the side is pointing to the right). Refer Table 1 which has the directivity of

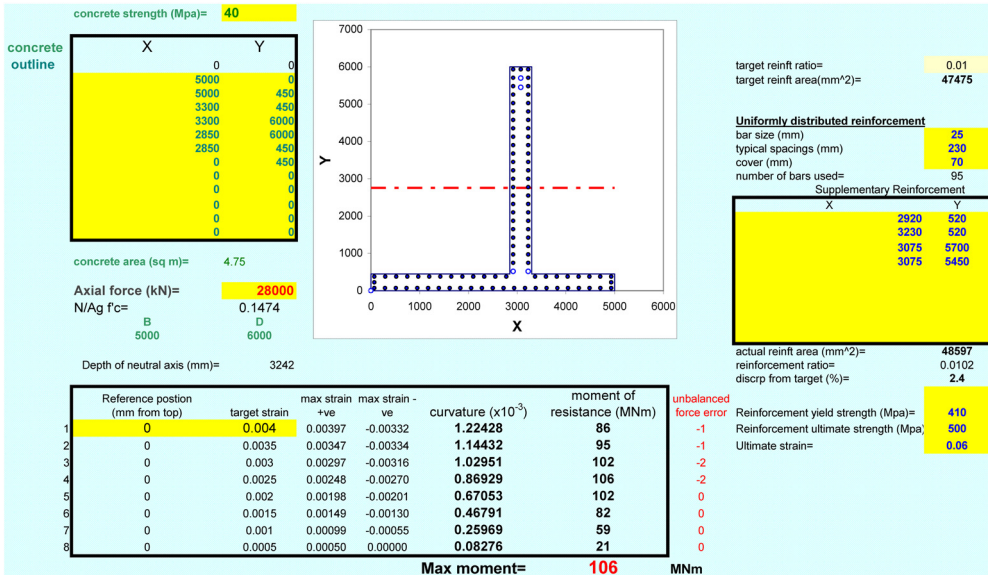

Fig. 2 Layout of page for user-interface

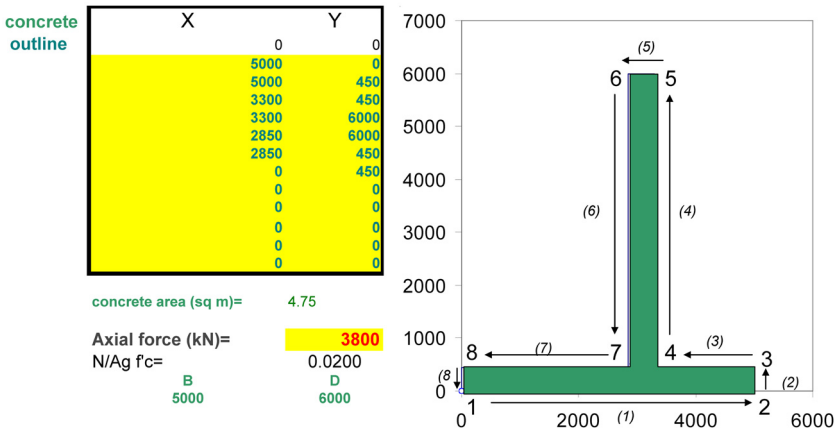

Fig. 3 Input of outline of wall cross-section

Table 1 Numbering of the sides, the nodes and directivity

Sides	Nodes	Offset of side from origin (mm)	Parallel to X or Y	Directivity of side
(1)	1 – 2	0	X	Positive (+1)
(2)	2 – 3	5000	Y	Positive (+1)
(3)	3 – 4	450	X	Negative (-1)
(4)	4 – 5	3300	Y	Positive (+1)
(5)	5 – 6	6000	X	Negative (-1)
(6)	6 – 7	2850	Y	Negative (-1)
(7)	7 – 8	450	X	Negative (-1)
(8)	8 – 1	0	Y	Negative (-1)

every side of the cross-section listed. The identified directivity facilitates calculations for the cross-sectional area and other geometrical properties in the later part of the program (Section 3.1).

2.2 Input of wall longitudinal reinforcement

First, the targeted longitudinal reinforcement ratio ρ_{sl} (sum of the areas of the reinforcement, A_{sl}, expressed as a fraction of the cross-sectional area of the concrete, A_g) is keyed in by the user. The value of A_{sl} is then calculated as reference information to guide design. In the example case study shown in Fig. 4, A_{sl} is approximately equal to 48,000 mm^2 for ρ_{sl} = 0.01.

The longitudinal reinforcement to be specified is of two types: (i) uniformly distributed reinforcement and (ii) supplementary reinforcement. Uniformly distributed reinforcement is specified by the *bar diameter*, *notional spacing* and *cover* (which is defined as the offset of the centre of the reinforcement from the surface of the concrete and is not to be confused with the usual definition of *cover* in the context of compliance with provisions for durability and fire-rating). Supplementary reinforcement is then specified bar by bar in the table shown in Fig. 4 where the X-Y positioning

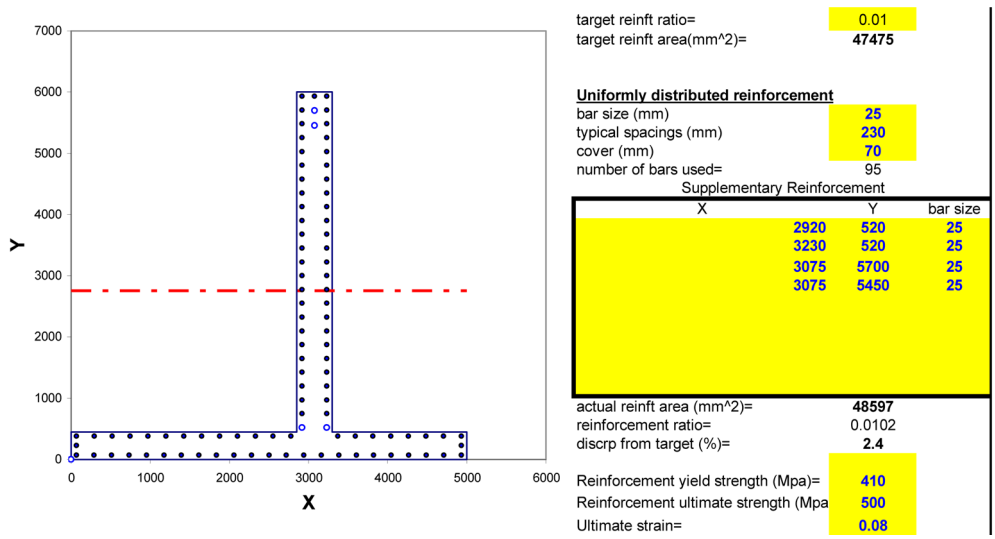

Fig. 4 Input of details of longitudinal reinforcement

and diameter of each bar is keyed in. The calculated values of A_{sl} and ρ_{sl}, and the discrepancy with the target values (shown at the top of the list) are then reported. Finally, the characteristic yield strength (f_{sy}), ultimate strength (f_{su}) and ultimate tensile strain (ε_{su}) of the reinforcement are keyed in by the user.

2.3 Summary of analysis results

When details of the cross-section and longitudinal reinforcement have been input into the program, computations are prompted by keying in the target strain at a reference position on the cross-section. For example, the target compressive strain (ε_c) at the upper extreme fibre of the cross-section (i.e., *zero* mm measured from the upper surface) can be specified. For poorly confined concrete, a nominal ε_c value of 0.004 is usually specified for the *damage control* limit state. Refer entry to the 1st row, 1st and 2nd column, of the table in Fig. 5. Listed alongside the input parameters are the maximum compressive (+ve) and maximum tensile (-ve) strains, the section curvature and the moment of resistance calculated from the program.

Further results associated with lower strain levels (in regular decrements down to zero strain) are listed on the 2nd-8th row of the table. The moment-curvature diagram is accordingly generated by the program as shown in Fig. 5. Note, the applied axial force is (N) is taken to be applied at the geometrical centre of the cross-section (mid-way between the extreme fibres) and is not necessarily at the centre of resistance. Thus, the moment of resistance which is taken about the geometrical centroid might have non-zero values at zero curvature when an axial force is applied. It is noted that the calculated *unbalanced forces* are listed on the right hand side of the table for reference by the user. Such error data are to indicate non-convergence in the computations should that occur in the computations.

	Reference postion (mm from top)	target strain	max strain +ve	max strain -ve	curvature (x10^{-3})	moment of resistance (MNm)	unbalanced force error
1	0	0.004	0.00394	-0.01090	**2.47322**	**76**	0
2	0	0.0035	0.00344	-0.01045	**2.31227**	**78**	0
3	0	0.003	0.00295	-0.00957	**2.08197**	**80**	-1
4	0	0.0025	0.00246	-0.00813	**1.76057**	**80**	0
5	0	0.002	0.00197	-0.00612	**1.34624**	**79**	-1
6	0	0.0015	0.00148	-0.00390	**0.89612**	**75**	0
7	0	0.001	0.00099	-0.00205	**0.50806**	**66**	0
8	0	0.0005	0.00049	-0.00093	**0.23835**	**34**	0
					Max moment=	**80**	**MNm**

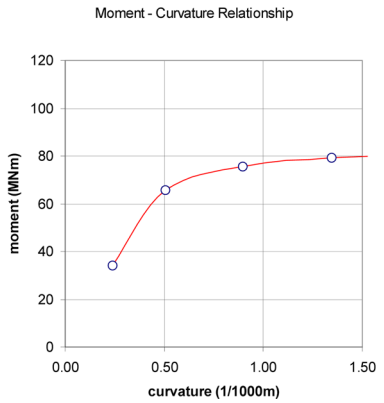

Moment curvature curve

Fig. 5 Analysis results summary

3. Programming of the computations

3.1 The fibre-elements

The basis of fibre-element modelling is to divide the concrete cross-section into very thin horizontal slices of uniform thickness ($t = 50$ mm was adopted in the illustrated examples). The fibre elements could be of variable widths except for rectangular cross-sections which have uniform widths. Whilst cross-sectional area and other geometrical properties are easy to calculate by hand, programming those calculations on spreadsheet is less straightforward. The following is a description of the programming strategy that has been adopted for calculating the width of each fibre element given the position of the nodes as defined by Cartesian co-ordinates.

The *directivity* and the *offset* of the vertical sides of the cross-section from the origin can be used for calculating the widths of the fibre-elements. It is noted that concrete is always on the left of the side which has been identified with a positive directivity (Table 1 and Fig. 3), and on the right of the side which has been identified with a negative directivity. If positive and negative directivity is represented by "+1" and "-1" respectively, then the arithmetic sum of the product of *directivity* and *offset* of the vertical side from the origin is automatically the width of the respective fibre elements. For example, consider fibre elements which constitute the flange of the wall are bounded by sides labeled as "2" and "8" respectively (Fig. 6(a)). The width of fibre elements in the flange as shown by the line identified as "*a*" in Fig. 6(a) is simply equal to: (+1)(5000) + (-1)(0) = 5000 mm; and width of fibre elements in the web as shown by the line identified as "***c***" is (+1)(3300) + (-1)(2850) = 450 mm. Similarly, the width of fibre elements in the web of the channel section as shown by the line identified as "*d*" in Fig. 6(b) is (+1)(3000) + (-1)(2550) = 450 mm. With the more complex configuration of a double-web in the upper part of the channel section (Fig. 6(b)), the total width of the webs (as represented by lines identified as "***e***") is simply the sum of the product of the *directivity* and *offset* for sides labeled as "2", "8", "6" and "4" which is (+1)(3000) + (-1)(2550) + (+1)(450) + (-1)(0) = 900 mm.

Once the width of every fibre-element in the cross-section has been identified, all geometrical properties of the cross-section such as the total area, position of the centroid and the second moment

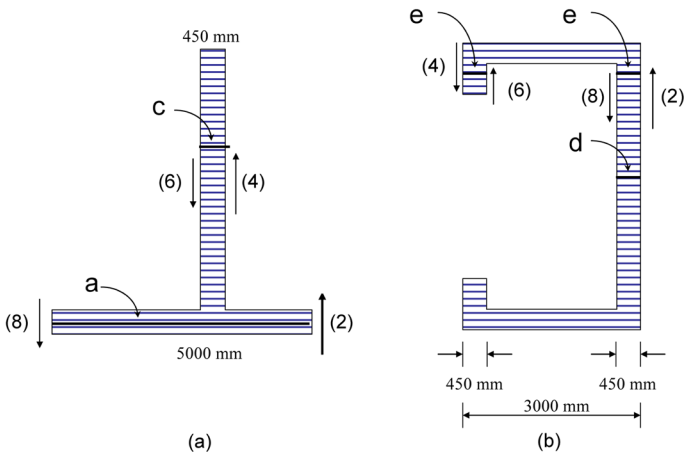

Fig. 6 Fibre-elements

of area can be calculated readily by numerical integration. Uniformly distributed reinforcements generated for each side of the cross-section are of uniform spacings which is guided by the notional spacing specified by the user. However, the actual reinforcement spacing could be less than the specified spacing and much depends on the dimensions of the cross-section. For example, there is always a bar positioned close to every corner of the cross-section irrespective of the spacing between the two corner bars. Programmers are cautioned to ensure that the same corner bars are not generated twice from the two sides meeting at the corner. The strategy adopted by the authors is to associate all corner bars with the horizontal sides only (which means that end bars from the vertical sides are omitted).

3.2 Stresses and strains

Computation commences with an initial strain profile which is constrained by the target strain specified by the user and an assumed position of the neutral axis. Given the initial strain profile, the strain for each fibre element can be found by linear interpolation. Stresses in both the concrete and steel are then calculated in accordance with the material stress-strain behaviour which is defined by Eqs. (1) and (2) for concrete and steel respectively. Eq. (1) was obtained by adapting the model developed originally by Mander *et al.* (1988) to concrete of poor confinement where maximum stress in the concrete is taken as the characteristic strength (f_c') whereas the strain at maximum stress is taken as 0.002. The earlier, more conservative, model presented by Park and Paulay (1975) could also be used (Fig. 7(a)). Eq. (2) which was cited by Priestley *et al.* (2007) has been modified to eliminate the *yield plateau* which only exists in the initial cycle of loading (Fig. 7(b)).

For poorly confined Grade 40 concrete

$$f_c = \frac{f_c' \cdot x \cdot r}{r - 1 + x^r} \quad \text{for} \quad \varepsilon_c < 0.004 \tag{1a}$$

where

$$x = \frac{\varepsilon_c}{0.002},\ r = \frac{E_c}{E_c - E_{sec}},\ E_{sec} = \frac{f_c'}{0.002} \tag{1b – 1d}$$

$$E_c = 5000\sqrt{f_c'} \ \text{(both } E_c \text{ and } f_c' \text{ in units of MPa)} \tag{1e}$$

For 400 MPa steel reinforcement :

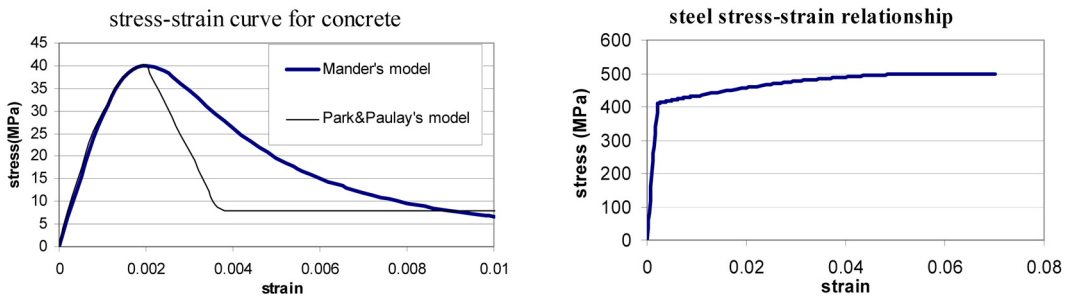

(a) Concrete (b) Steel

Fig. 7 Stress-strain relationships for concrete and steel

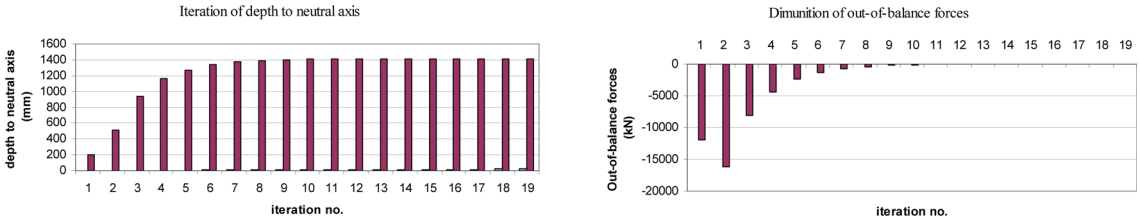

(a) Depth to neutral axis (b) Out-of-balance forces

Fig. 8 Samples of results from iterative computations

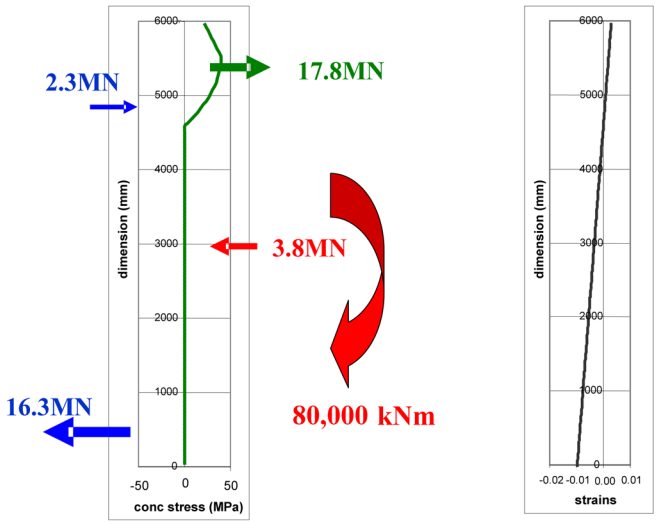

(a) Stress Diagram (b) Strain Diagram

Fig. 9 Example stress-strain diagrams obtained from an iterative procedure

$$f_s = E_s \cdot \varepsilon_s \quad \text{for} \quad \varepsilon_s < \varepsilon_{sy}\,(\varepsilon_{sy} = 0.002) \tag{2a}$$

$$f_s = f_{su} - (f_{su} - f_{sy})\left(\frac{\varepsilon_{su} - \varepsilon_s}{\varepsilon_{su} - \varepsilon_{sy}}\right)^2 \tag{2b}$$

For the Grade 40 concrete adopted in the example case studies, the value for f_c' was taken as 40 MPa and the value of E_c was estimated to be 30 GPa. For the 400 MPa steel the value for f_{sy}, f_{su} and ε_{su} was taken as 410 MPa, 500 MPa and 0.08 respectively. These parameter values have been used in all worked examples illustrated in the paper.

The forces associated with the concrete material in each fibre element is then obtained as the product of the width of the element, its thickness (50 mm) and the concrete stress identified for the element. Likewise, forces associated with reinforcements included in each element are also calculated.

Forces calculated for the assumed strain profile are then summed to check for equilibrium in an iteration. The out-of-balance forces which are indicative of errors in the assumed strain profile are then used to adjust the position of the neutral axis in the next step of the iteration. It is shown with the example case study that convergence of the position of the neutral axis is achieved after some *six* iterations whilst the program allows up to *nineteen* iterations to be undertaken (Figs. 8(a) and

8(b)). In most cases the position of the neutral axis will have converged and the out-of-balance forces diminished to a negligible level at the conclusion of the analysis.

Upon convergence of the position of the neutral axis, the tensile and compressive forces are used for calculating the total moment of resistance about the section geometrical centroid (Fig. 9). Meanwhile, the curvature of the section is determined by dividing the difference of the strains of the extreme fibres by the total depth of the concrete cross-section.

3.3 Generation of moment-curvature relationships

In summary, the moment-curvature pair of results is obtained using the calculation procedure described above based initially on the target strain that has been specified by the user. This is done in one spreadsheet. Similar moment-curvature pairs of results are calculated for lower levels of strains using separate spreadsheets (refer table in Fig. 5 for the listing of the results). These results are used collectively for constructing the moment-curvature diagram of Fig. 5. Further examples of moment-curvature diagrams constructed for a range of cross-sections are presented in the next section in Fig. 10(a)-10(d).

4. Example moment curvature relationships

Moment-curvature diagrams have been calculated using the program for four different types of

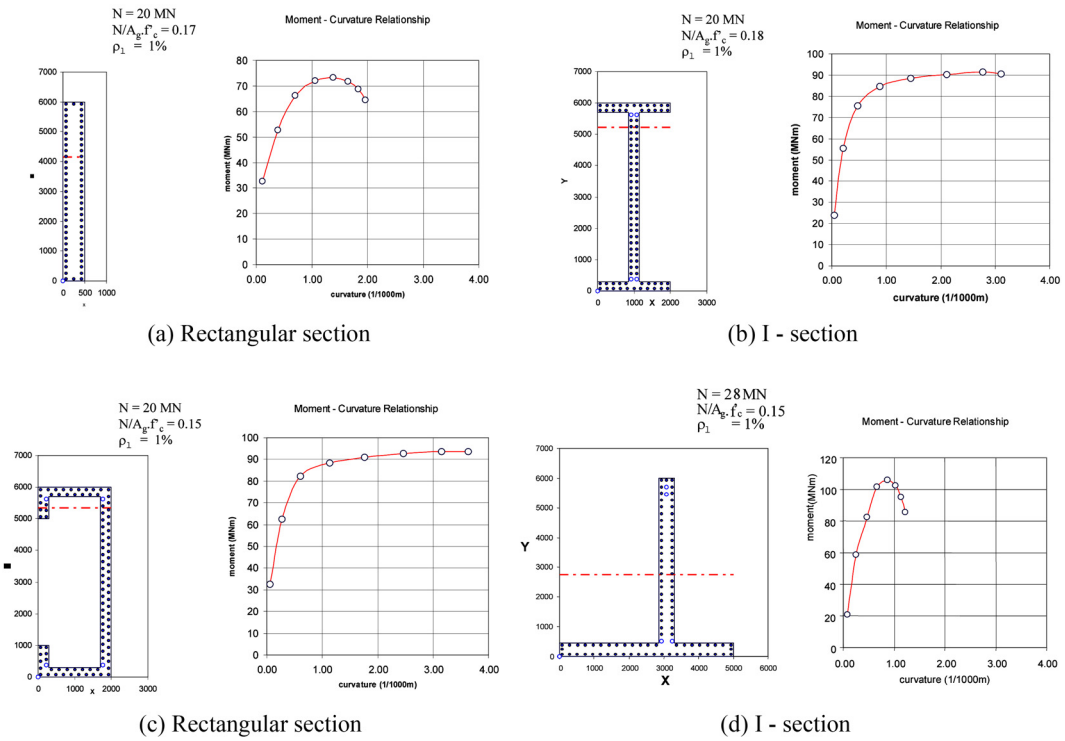

(a) Rectangular section (b) I - section

(c) Rectangular section (d) I - section

Fig. 10 Example computed moment – curvature relationship

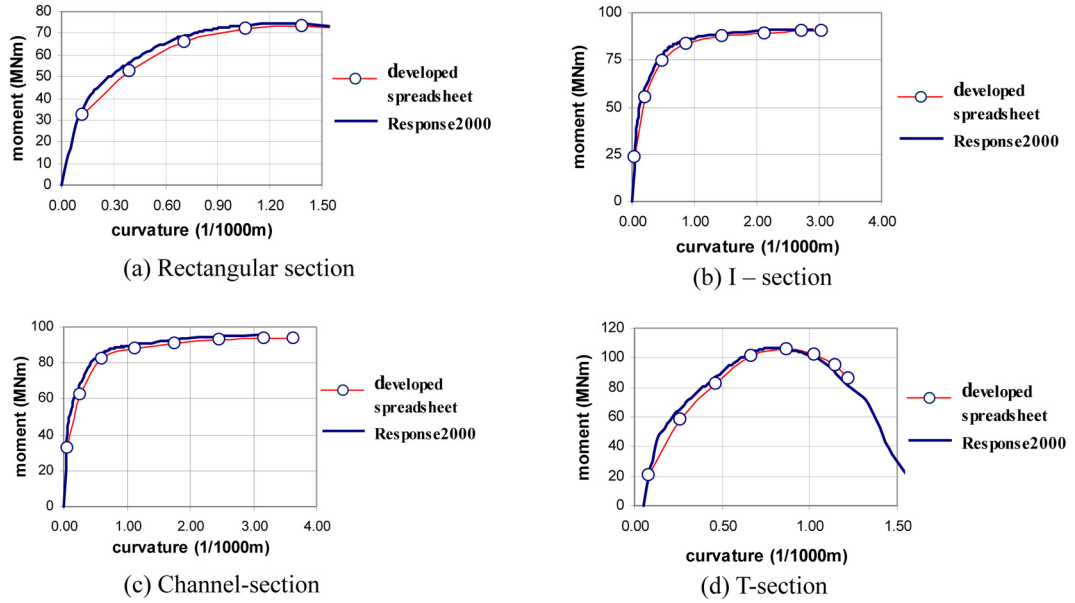

(a) Rectangular section (b) I – section

(c) Channel-section (d) T-section

Fig. 11 Comparison with program Response 2000

cross-sections: (i) rectangular section, (ii) I – section, (iii) channel section and (iv) T-section for axial pre-compression parameter ($N/A_g\ f_c'$) in the range 0.15-0.18 and a reinforcement ratio equal to 0.01. Moment-curvature diagrams were also constructed using computer program RESPONSE 2000 to validate the accuracy of the developed spreadsheet. Comparison of the moment-curvature diagrams is presented in Fig. 11.

Whilst a similar moment of resistance was estimated for all the cross-sections considered, it is interesting to see the significant differences in the shape of the moment-curvature diagrams constructed. Clearly, the I-section and the channel section are noticeably more ductile than the other section configurations (Figs. 10(a)-10(d)).

Information on the ductility of the cross-section can be very critical to the potential seismic resistant capacity of a structural wall. Yet, conventional calculation procedures as stipulated in standards and codes of practice for the design of reinforced concrete walls and columns are mainly about calculating the moment of resistance whilst there is typically no requirement for estimating the associated curvature at yield.

Further analyses of the wall cross-section were then carried out based on varying the axial pre-compression ratio ($N/A_g\ f_c'$ varying from 0.02 to 0.17). In each case, the notional yield curvature (ϕ_y) is identified and the associated flexural stiffness (M_y/ϕ_y) obtained by graphical construction of the bi-linear model as shown in Figs. 12 and 13. It is shown that the calculated flexural stiffnesses were very sensitive to the level of pre-compression whereas the value of ϕ_y was very well constrained within the range: 0.7-0.9 km^{-1} which is consistent with estimates by Eq. (3) as recommended by Priestley *et al.* (2007). A summary of the calculated stiffnesses in comparison with the gross-sectional stiffnesses *EI* are shown in Table 2. The last column of the table shows the calculated effective stiffness ratios which are very sensitive to the level of pre-compression and are in good agreement with estimates by Eq. (5.7) in Paulay and Priestley (1992). Thus, any attempt to generalize the estimate for the effective stiffness without undertaking moment-curvature analysis

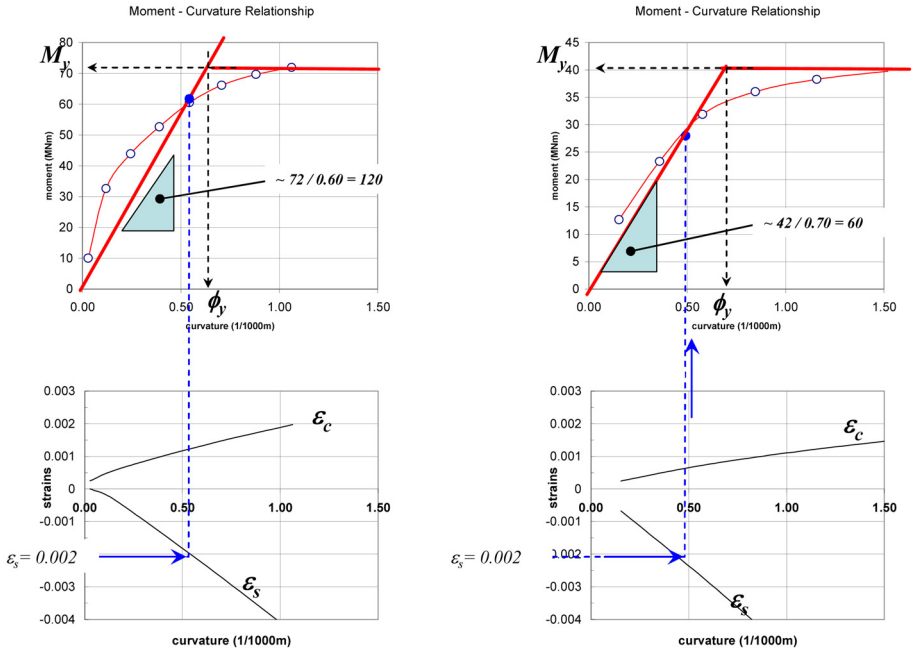

(a) N/A_g. $f'_c = 0.17$ (b) N/A_g. $f'_c = 0.025$

Fig. 12 Notional yield curvature and effective stiffness (rectangular section)

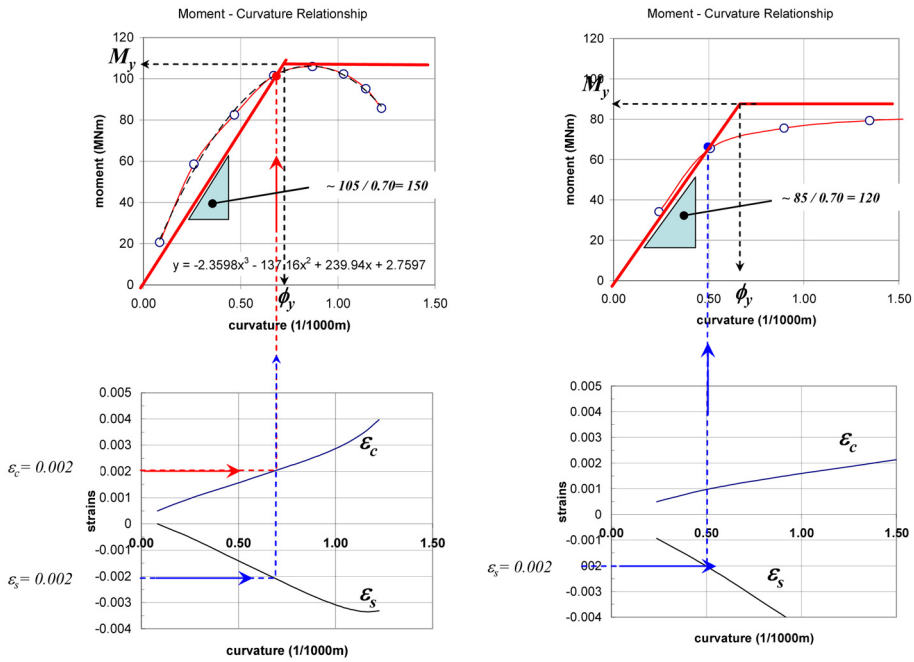

(a) N/A_g. $f'_c = 0.15$ (b) N/A_g. $f'_c = 0.02$

Fig. 13 Notional yield curvature and effective stiffness (T - section)

Table 2 Flexural stiffnesses at notional yield

Section type	N/Ag f_c'	M_y/ϕ_y (MNm^2 × 10^3)	EI (MNm^2 × 10^3)	(M_y/ϕ_y)/EI
(a) Rectangular	0.170	120	270	0.44
(b) Rectangular	0.025	60	270	0.23
(c) T – section	0.150	150	510	0.29
(d) T - Section	0.020	120	510	0.24

could result in significant errors.

$$\phi_y = \frac{2\varepsilon_y}{l_w} = \frac{2(0.0025)}{6} = 0.00083 \text{ m}^{-1} \quad \text{or} \quad 0.83 \text{ km}^{-1} \tag{3}$$

where l_w is wall length.

5. Applications in seismic design and assessment

The limiting curvature values obtained from the spreadsheet program can be used for estimating the displacement capacity of structural walls. The calculated displacement capacity of a wall can be compared against the seismic displacement demand as indicated from the elastic displacement response spectrum of the earthquake, if the estimates are expressed in terms of the effective displacement (Δ_e) of the building (Priestley *et al.* 2007).

For a *multi-degree-of-freedom* system, Δ_e is defined as the displacement of an equivalent *single-degree-of-freedom* system with natural period and damping properties matching that of the fundamental mode of natural vibration of the building. For buildings in which the lateral resistance is provided mainly by structural walls, Δ_e is typically the displacement of the building at around 70% up its height (which is defined herein as the effective height, h_e). The effective displacement capacity of a structural wall can be decomposed into two components: (i) effective displacement at notional yield (Δ_{ey}) and (ii) additional effective post-yield displacement to reach a certain damage control limit state (Δ_{ep}).

In theory, the value of Δ_{ey} should be calculated from the curvature profile up the height of the wall by double-integration. However, it is recommended that a more realistic estimate of Δ_{ey} can be obtained by the much simpler expression of Eq. (4) which is based on assuming a linear curvature profile. It was found that errors associated with the linearization are generally small and are mostly offset by additional displacement due to tension shifts (Priestley *et al.* 2007).

$$\Delta_{ey} = \phi_y \frac{h_e^2}{3} \tag{4}$$

Additional post-yield displacement can be obtained using Eq. (5) which is based on modelling a plastic hinge rotation at the base of the wall (Priestley *et al.* 2007).

$$\Delta_{ep} = (\phi_m - \phi_y) \cdot L_p \left(h - \left(\frac{L_p}{2} - L_{sp} \right) \right) \tag{5a}$$

where

$$L_p = K_p \cdot h_e + 0.1 l_w + L_{sp} \tag{5b}$$

Table 3 Effective displacement capacity of structural walls

Section type	$N/A_g\ f_c'$	Δ_{ey} (mm)	Δ_{ep}(mm)	Δ_e(mm)
(a) Rectangular	0.170	78	32	110
(b) Rectangular	0.025	72	88	160
(c) T – section	0.150	77	13	90
(d) T – Section	0.020	72	48	120

$$K_p = 0.2\left(\frac{f_{su}}{f_{sy}} - 1\right) \leq 0.08 \tag{5c}$$

$$L_{sp} = 0.022 \cdot f_{ya} \cdot d_{bl} \tag{5d}$$

l_w is wall length, $f_{ya} = f_{sy}$ 410 MPa, f_{su} = 500 MPa, and d_{bl} is diameter of the longitudinal reinforcement.

Table 3 provides a listing of the effective displacement capacity of walls (of rectangular and T sections) which are 25 m high and providing lateral support for 8 storey buildings. The effective height h_e is assumed to be 17.5 m (= 0.7 × 25). The estimated displacement at yield is very similar across all the cases considered but there are significant differences with the post-yield displacement capacity based on the damage control limit state. As expected, T-section walls which are subject to a pre-compression ratio of 0.15 are estimated to have the most limited displacement capacity (90 mm). By contrasts, walls of the rectangular cross-sections with a nominal pre-compression ratio of 0.025 have a much more generous displacement capacity of 160 mm. This significant difference in the displacement capacity would not have been captured by the conventional force-based procedure currently stipulated in standards and codes of practices. The displacement profile of the wall at *yield* and limit state of *damage control* can be expressed in terms of the respective effective displacement as shown by Eqs. (6a) and (6b). Profiles representing each of the cases listed in Table 3 are shown in Figs. 14(a)-14(d).

$$\Delta_{iy} = \Delta_{ey}(1.5)\left(\frac{h_i}{h_e}\right)^2\left(1 - \frac{h_i}{3H}\right) \tag{6a}$$

$$\Delta_{ip} = \Delta_{ep}\frac{h_i - \left(\frac{L_p}{2} - L_{sp}\right)}{h_e - \left(\frac{L_p}{2} - L_{sp}\right)} \tag{6b}$$

where Δ_{iy} and Δ_{ip} are displacements at height h_i.

Finally, the effective displacement capacity of the structural walls as listed in Table 3 are compared with the *peak displacement demand* that has been estimated with a notional peak ground acceleration of 0.08 g. Whilst this level of seismic hazard has been stipulated for the capital cities of Melbourne, Sydney and Canberra by the Australian Standard for seismic actions (AS1170.4 2007), this case study is not intended to be restricted to any particular country and can be applied in any parts of the world which are characterized by conditions of low-moderate seismicity with diffused seismic sources. The *peak displacement demand* (*PDD*) in units of *mm* can be estimated in accordance to the Australian Standard (AS1170.4 2007) using Eq. (7) which is parameterized by the *hazard factor* Z (representing the notional peak ground acceleration on rock sites in units of g's for a return period of 500 years), the return period factor R_p (which is normalised to unity at the

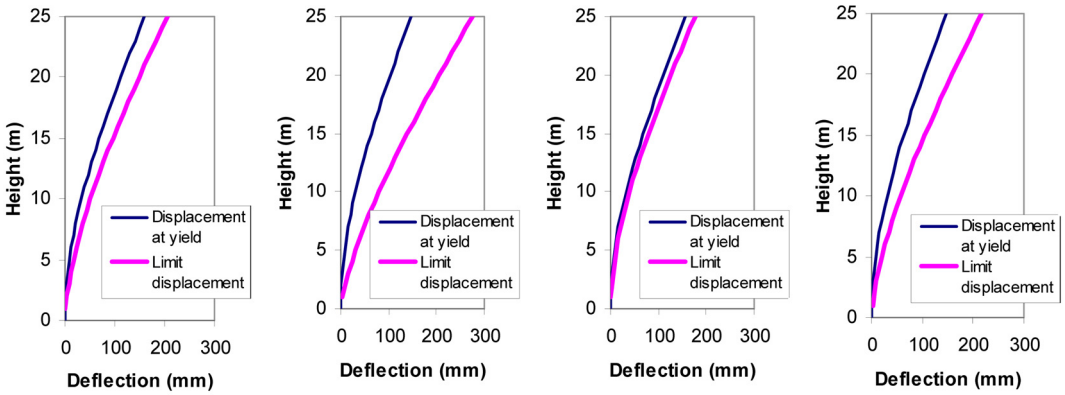

Fig. 14 Displacement profile at yield and damage control limit state

Table 4 Estimates of *Peak Displacement Demand* for Z = 0.08

Site class	Site factor F_v	500 years return period (Rp = 1.0) *PDD* in units of mm	2500 years return period (Rp = 1.8) *PDD* in units of mm
B	1.00	25	45
C	1.40	35	65
D	2.25	60	105
E	3.50	90	160

reference return period of 500 years) and site amplification factor F_v (which is normalized to unity for average rock conditions). The value of "1.5" in Eq. (7) is the corner period value of the response spectrum model adopted by AS1170.4 (2007) for all site classes. Thus, Eq. (7) provides estimates of the highest displacement demand of single-degree-of-freedom systems for 5% damping.

$$PDD = 1.8(750R_pZ)F_v\frac{1.5}{2\pi} = 320R_pZF_v \quad (PDD \text{ is in units of mm}) \tag{7}$$

The comparison of the wall displacement capacity (Table 3) with the seismically induced displacement demand (Table 4) shows that 25 m high structural walls considered in this study would be able to accommodate *Peak Displacement Demand* consistent with a *hazard factor* of 0.08g except for Class D & E sites for a return period of 2500 years. The displacement capacity at yield is never significantly exceeded for all site classes with a return period of 500 years. It should be noted that buildings are assumed to be regular so that the effects of torsion can be neglected.

6. Conclusions

This paper introduces a transparent program written on EXCEL spreadsheets for analyzing the moment-curvature relationships of reinforced concrete cross-sections of arbitrary geometry. Input parameters to be keyed in by the user are the co-ordinates of the corners of the cross-section, the

reinforcement diameter and their notional spacing, and the characteristic strengths of concrete and steel. Output moment-curvature diagrams and displacement profiles are provided instantaneously by the program. Key features with the programming are described to facilitate readers developing a program of their own customizing individual requirements. Example moment-curvature diagrams have been generated for a range of structural wall cross-sections : *rectangular*, *I*, *T* and *channel*.

Curvature at notional yield and user-specified damage control limit states were obtained by fitting bi-linear relationships to the calculated results. The calculated limiting curvature values were used to estimate displacement profiles up the height of the wall for comparison with the seismically induced displacement demand for given values of the *hazard factor*, *return period factor* and *site factor*. It is shown in the comparative analysis that 25 m high structural walls with a range of cross-sections considered in this study (and with pre-compression ratio of up to 0.17 and a reinforcement ratio of 0.01) would be able to accommodate the *Peak Displacement Demand* consistent with a *hazard factor* of 0.08g except for Class D & E sites for a return period of 2500 years. The displacement capacity at yield is never significantly exceeded for all the site classes with a return period of 500 years.

References

AS1170.4 (2007), *Structural design actions. Part 4: Earthquake actions in Australia,* Standards Australia, Sydney, NSW.

CUMBIA (2007), Montejo, L.A. and Kowalsky, M.J., *Set of codes for the analysis of reinforced concrete members,* Report No. IS-07-01, Constructed Facilities Laboratory, North Carolina State University, Raleigh, NC.

FEAP (1998), Taylor, R.L., *A finite element analysis program. User's manual : version 7.1,* Department of Civil & Environmental Engineering, University of California, Berkeley.

Mander, J.B., Priestley, M.J.N. and Park, R. (1988), "Observed stress-strain behaviour of confined concrete", *J. Struct. Eng. - ASCE,* **114**(8), 1827-1849.

Monti, G. and Spacone, E. (2000), "Reinforced concrete fiber beam element with bond-slip", *J. Struct. Eng. - ASCE*, **126**(6), 654-661.

Park, R. and Paulay, T. (1975), *Reinforced concrete structures*, John Wiley & Sons Inc.

Paulay, T. and Priestley, M.J.N. (1992), *Seismic design of reinforced concrete and masonry buildings*, John Wiley & Sons, Inc.

Priestley, M.J.N., Calvi, G.M. and Kowalsky, M.J.N. (2007), *Displacement-based seismic design of structures*, IUSS Press, Pavia, Italy.

RESPONSE (2000), Bentz, E.C., *Sectional analysis of reinforced concrete members,* PhD thesis, University of Toronto.

Spacone, E., Filippou, F.C. and Taucer, F.F. (1996a), "Fibre beam-column model for non-linear analysis of R/C frames. Part 1: Formulation", *Earthq. Eng. Struct. Dyn.,* **25**, 711-725.

Spacone, E., Filippou, F.C. and Taucer, F.F. (1996b), "Fibre beam-column model for non-linear analysis of R/C frames. Part 2: Applications", *Earthq. Eng. Struct. Dyn.,* **25**, 727-742.